International Journal of Bridge Engineering (IJBE), Vol. 5, No. 3, (2017), pp. 31-52

PEDESTRIAN SUSPENSION BRIDGE NUMERICAL MODEL RESPONSE TO LOAD SIMULATIONS

Yi Mao[1] and Jeffrey A. Laman[2]

[1] Modjeski and Masters Inc., Washington, DC USA
[2] The Pennsylvania State University, Dept. of Civ. and Env. Engrg., University Park, PA USA
e-mail: yim9127@gmail.com, jlaman@psu.edu

ABSTRACT: During rainy seasons, rural communities around the world become isolated from health care, education and other essential services due to flooding. Pedestrian suspension bridges are built to provide these communities with access to their basic needs. However, dynamic response problems may occur due to low stiffness, low mass and low damping of these bridges.

The present study utilized a scaled, physical suspension bridge model to obtain dynamic response data that was in turn utilized to develop and calibrate a numerical bridge modeling methodology. The calibrated modeling methodology was employed to complete several dynamic analysis simulations under more complex load cases and combinations than have previously been studied. Simulations in the present study include seventeen pedestrian load combinations, one animal load combination and one handcart load combination. In addition, an investigation into the influence of a bystander on bridge dynamic response was conducted through modeling a human bystander.

The present study observed that the peak response induced by a jogger is twice the response of a walker, while a bicycle induces a 77 percent smaller response than the walker. The most critical combination for two pedestrians occurs when they enter the bridge together at the same time and maintain the same pace. It was also observed that the existence of a bystander decreases the vertical response near the bystander location while the lateral response is minimally affected.

KEYWORDS: Bridges; Dynamic; Pedestrian; Simulation; Suspension.

1 INTRODUCTION

A suspension pedestrian bridge is a bridge designed exclusively for pedestrians, and in some cases cyclists and animal traffic, rather than vehicular traffic. Several organizations around the world construct suspension pedestrian bridges in rural communities using simple and inexpensive local materials. Those over impassable rivers provide isolated communities with access to health care, education and other essential services during rainy seasons. For such bridges

with low stiffness, mass, and damping, serviceability is of concern because a serviceability failure may result in pedestrians choosing not to use the bridge.

To better predict the dynamic responses of a suspension pedestrian bridge, the present study calibrated a full-scale numerical bridge model using the obtained frequencies of a scaled physical model. A study of dynamic simulation under different load cases was subsequently conducted based on the calibrated numerical model design.

Load cases developed in the present study include pedestrian walking loads, jogging loads and cycling loads. Different load combinations limited to two pedestrians were investigated. In addition to load cases and combinations consisting of pedestrians, load cases and combinations including animal footfall forces and handcart loads were also investigated. Finally, an investigation into the influence of a bystander on bridge dynamic responses was conducted.

1.1 Load case functions

A pedestrian bridge is subjected to many types of pedestrian loading, with the most common being walking pedestrians. However, there are other pedestrian activities that may induce more a severe response. Pedestrian activity evaluated in the present study consists of walking, jogging, and cycling. These loads were modeled through a time history analysis to determine the dynamic responses of a pedestrian bridge.

Figure 1 presents pedestrian walking force vs. time in both vertical and lateral directions and Figure 2 presents pedestrian jogging force vs. time. These load functions were developed based on research conducted by Andriacchi, Wheeler, Galbraith and Barton [1, 2, 3]. Pedestrian walking speed is 1.2 m/s and jogging speed is 3 m/s.

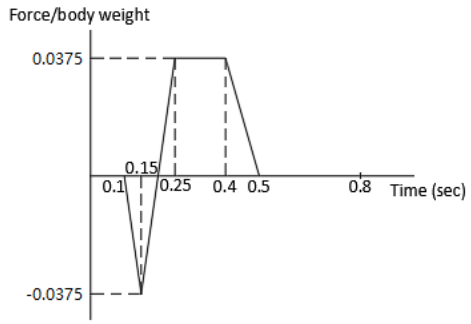

a) lateral direction

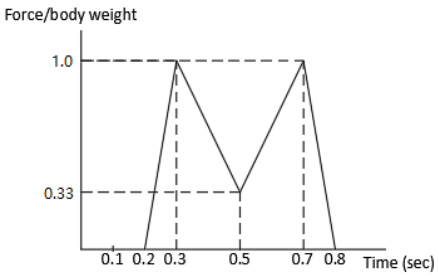

b) vertical directionTime

Figure 1. Time function for pedestrian walking force

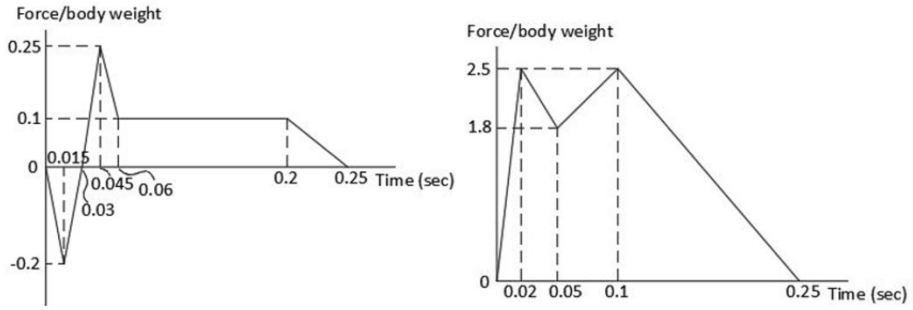

a) lateral direction b) vertical direction

Figure 2. Time function for pedestrian jogging force

Pedestrian cycling forces are modeled as two moving point loads with a constant distance of 1 m, each representing one wheel. Figure 3 presents the default time function embedded in SAP2000 that is applied to each wheel load in a time history moving load analysis [4]. Pedestrian cycling speed for the present study is taken as 3.5 m/s. Loads induced by a handcart exhibit the same pattern as a cycling force and is automatically created by SAP2000 as presented in Figure 3.

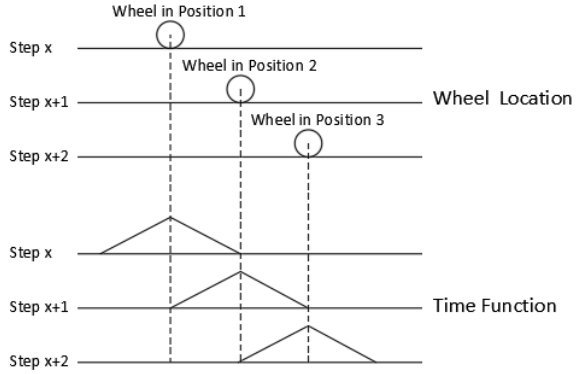

Figure 3. Time function for cycling live load [4]

Two additional, common load cases were considered to investigate the dynamic response of a pedestrian suspension bridge: four-legged animal and handcart loads. Figure 4 presents the animal load time-history function developed based on experimental results reported by Bobbert and Merkens [5, 6].

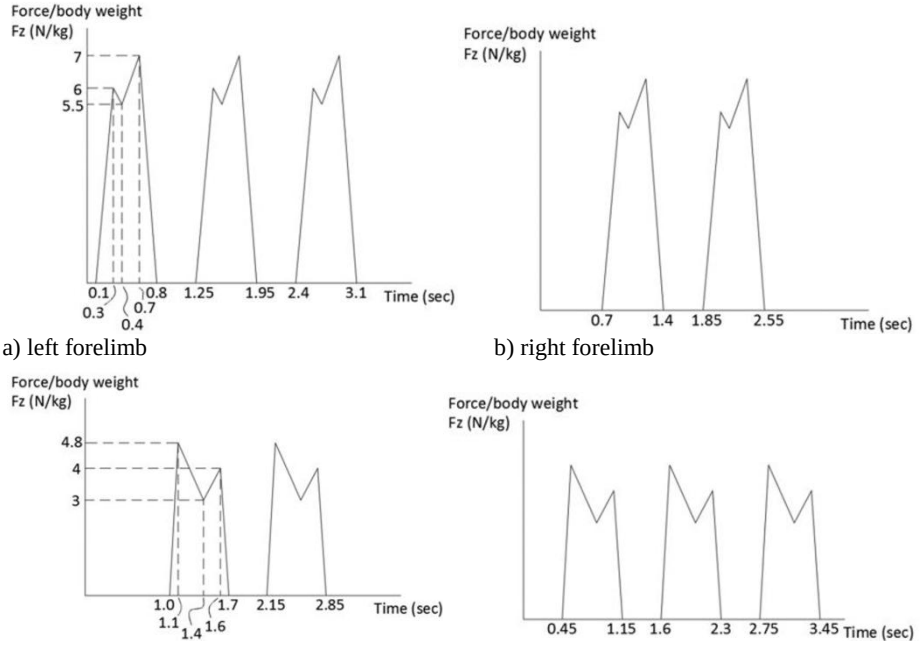

a) left forelimb b) right forelimb

c) left hindlimb d) right hindlimb

Figure 4. Time function for vertical animal force of each limb

1.2 Modelling a Bystander

A simple method to model a stationary person is to add additional mass to the structure. However, the mass-only model cannot reflect a significant increase in damping due to the bystander. Figure 5 presents five biomechanical models employed in the present study to investigate the influence of a bystander on the dynamic response of a pedestrian suspension bridge. These models were developed to fit experimental results [7, 8, 9, 10]. The dynamic characteristics of the five models are presented in Table 1.

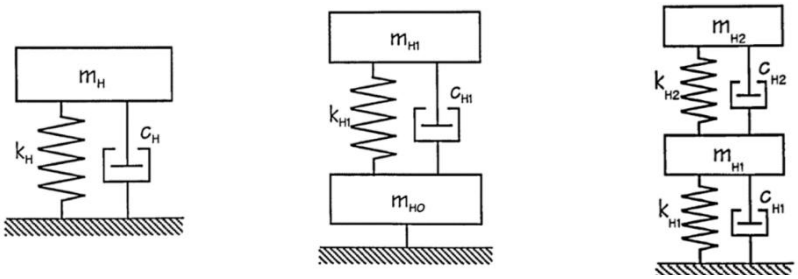

a) SDOF human body model without non-vibrating mass

b) SDOF human body model with non-vibrating mass

c) MDOF human body model using a 2-DOF system

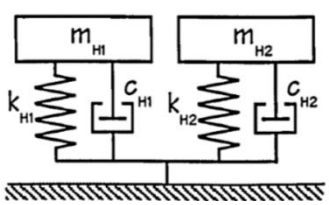

c) MDOF human body model using a 2-SDOF system

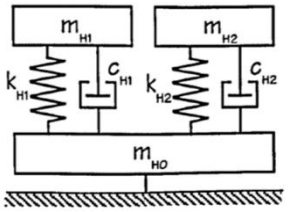

d) MDOF human body model using a 2-SDOF system with non-vibrating mass

Figure 5. Biomechanical models of a bystander [7]

Table 1. Characteristics of bio-mechanical models of a bystander [7]

Model	Spatial properties	Modal properties
damped SDOF model [8]	m_H = 86.2 kg k_H = 85.25 kN/m c_H = 1.72 kNs/m	f_1 = 5.0 Hz ζ_1 = 32%
2-SDOF model [9]	m_{H1} = 36.3 kg k_{H1} = 28.45 kN/m c_{H1} = 474 Ns/m	f_1 = 4.5 Hz ζ_1 = 23%
	m_{H2} = 12.5 kg k_{H2} = 15.03 kN/m c_{H2} = 271 Ns/m	f_2 = 5.5 Hz ζ_2 = 31%
SDOF model with non-vibrating mass [10]	m_{HO} = 4.1 kg	-
	m_{H1} = 46.7 kg k_{H1} = 44.115 kN/m c_{H1} = 1.522 kNs/m	f_1 = 4.9 Hz ζ_1 = 53%
2-SDOF model with non-vibrating mass [10]	mHO = 5.6 kg	-
	m_{H1} = 36.2 kg k_{H1} = 35.007 kN/m c_{H1} = 815 Ns/m	f_1 = 4.9 Hz ζ_1 = 36%
	m_{H2} = 8.9 kg k_{H2} = 33.254 kN/m c_{H2} = 271 Ns/m	f_2 = 9.7 Hz ζ_2 = 44%

2 NUMERICAL MODEL

A scaled, laboratory, physical model [11] was used to study pedestrian suspension bridge dynamic behavior and to calibrate numerical models that better reflect actual bridge construction. Figure 6 presents the SAP2000 numerical model design details. The suspenders that connect the main cable to the deck are modeled as undeformed cable elements. The main cables are modeled as cable elements based on the maximum vertical sag in the deformed shape. Decking boards are modeled as curved frame members with end rotation fully released. Independent gap elements, allowing compressive force only, model boundary conditions between the deck and abutments because movement of the deck end construction is restricted by an approach ramp with a small gap. The stiffness and gap element opening was calibrated using frequencies of the

scaled physical model that were obtained through dynamic tests. Table 2 presents calibration results for different mode shapes and Figure 7 presents all mode shapes that were considered.

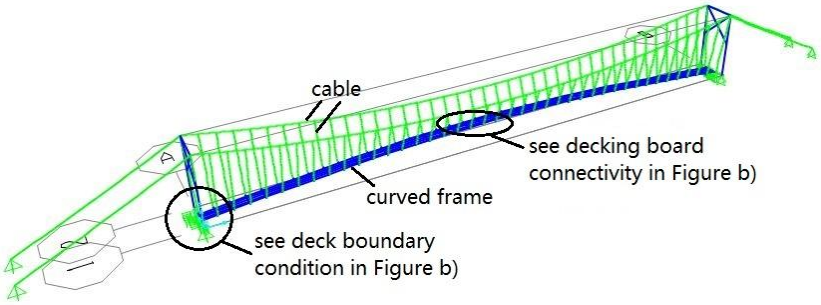

a) 40 m bridge numerical model

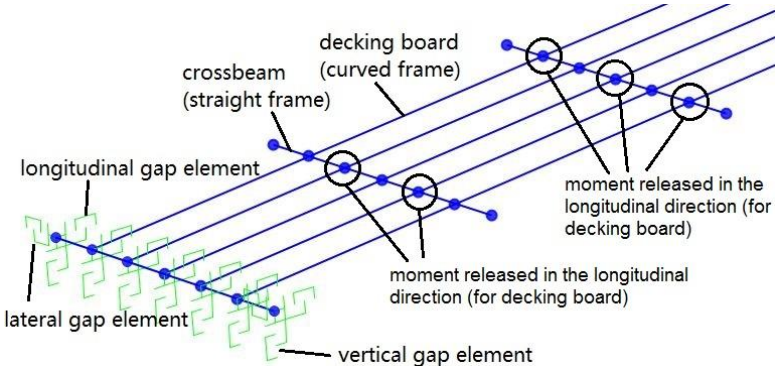

b) detailed boundary condition and member connectivity

Figure 6. 40 m span bridge numerical model built in SAP2000

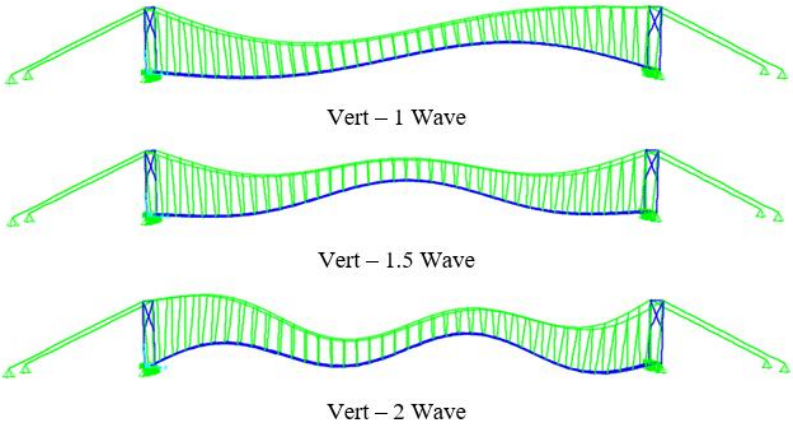

Figure 7. Vertical mode shapes

Table 2. Calibration results

Mode Shape	Physical Scaled Model Frequencies (Hz)	Numerical SAP2000 Model Frequencies (Hz)	Percent Difference
vertical – 1 sine wave	0.447	0.534	19.5%
vertical – 1.5 sine wave	1.04	0.999	3.94%
vertical – 2 sine wave	1.16	1.08	6.90%

3 DYNAMIC SIMULATION

A nonlinear, direct-integration, time-history analysis was conducted to determine the dynamic responses under each of the load cases and combinations. The numerical model response was evaluated on the basis of vertical velocity, vertical acceleration, and lateral acceleration at seven target points for dynamic response evaluation (Figure 8) which are the centers of every six-meter deck section labeled as 3D3, 3D9, 3D15, 3D21, 3D27, 3D33, and 3D38.

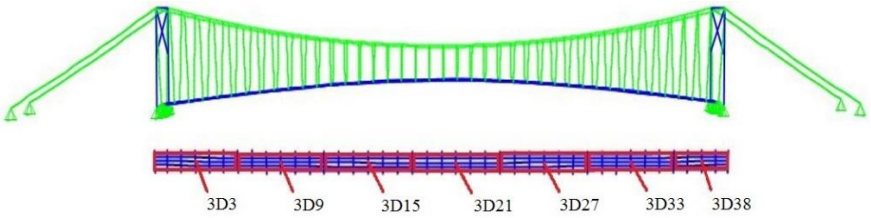

Figure 8. Target points evaluated for time history analysis

The pedestrian bridges that are the focus of the present study are commonly constructed to serve rural communities of developing countries for access to basic services. Therefore, it is likely not feasible to construct bridges that meet standards set by developed countries. It is also expected that pedestrians will modify their expectations of bridge performance in a developing country. Based on these criteria, serviceability limits are in reference to previous publications [12, 13] that explored human tolerance levels to vibrations. See Table 3 for the limits.

Table 3. Serviceability limits for the present study

Evaluation Term	Peak
vertical velocity (mm/s)	32
vertical acceleration (mm/s^2)	2250
lateral acceleration (mm/s^2)	1800

Table 4 presents the seventeen simulations used to conduct the study on pedestrian load cases and combinations. Designations for numerical models were defined according to study parameters – either the time offset or the meeting location. The simulations are confined to a 40 m bridge with five

percent sag. Table 4 also presents the meeting time for each load combination, which provides a reference while discussing the time history results. Table 5 presents two another load cases defined by an animal load and a handcart load.

Table 4. Pedestrian load cases and combinations

Load Case/ Combo	Description	Time Offset (sec)	Meeting Location	Meeting time (sec)	Designation
1PW	One pedestrian walks across the bridge.	/			40-5-1PW
1PJ	One pedestrian jogs across the bridge.				40-5-1PJ
1PC	One pedestrian cycles across the bridge.				40-5-1PC
2WS	Two pedestrians walk across the bridge from the same end.	1	/	/	40-5-2WS-1
		3			40-5-2WS-3
		5			40-5-2WS-5
		8			40-5-2WS-8
		12			40-5-2WS-12
2WD	Two pedestrians walk across the bridge from different ends.	/	3D9	25.5	40-5-2WD-9
			3D21	17	40-5-2WD-21
			3D33	27	40-5-2WD-33
WJS	One pedestrian walks across the bridge from the left end; another pedestrian jogs across the bridge from the same end.	/	3D9	7	40-5-WJS-9
			3D21	17	40-5-WJS-21
			3D33	27	40-5-WJS-33
WJD	One pedestrian walks across the bridge from the left end; another pedestrian jogs across the bridge from the right end.	/	3D9	10	40-5-WJD-9
			3D21	17	40-5-WJD-21
			3D33	27	40-5-WJD-33

Table 5. Animal load case and handcart load combination

Load case interpretation	Designation
An animal walks across the bridge with a speed of 1.1 m/s.	40-5-AnimalWalk
A pedestrian pushes a handcart with 22.7 kgf cargo.	40-5-HC

The present study also conducted a parametric study to evaluate the influence of bystanders on the dynamic properties and responses of pedestrian suspension bridges. Five different human bystander models described in section 1.2 were studied. The location of the bystander was limited to the midpoint and the quarter-point of the bridge. Dynamic response data is based on a single pedestrian walking across a 40 m bridge with five percent sag. The results are compared to response data of the bridge without a bystander. Table 6 presents designations for bridge models.

Table 6. Bridge models for parametric study on bystanders

Bystander Model Type	Bystander Location	Designation
no bystander	midpoint	40-5
modeled as additional mass		40-5-Mass-M
SDOF without non-vibrating mass (Figure 5 a)		40-5-SDOF-A-M
SDOF with non-vibrating mass (Figure 5 b)		40-5-SDOF-B-M
a 2-DOF system (Figure 5 c)		40-5-MDOF-A-M
a 2-SDOF system (Figure 5 d)		40-5-MDOF-B-M
a 2-SDOF system with non-vibrating mass (Figure 5 e)		40-5-MDOF-C-M
modeled As Additional Mass	quarter-point	40-5-Mass-Q
SDOF without non-vibrating mass (Figure 5 a)		40-5-SDOF-A-Q
SDOF with non-vibrating mass (Figure 5 b)		40-5-SDOF-B-Q
a 2-DOF system (Figure 5 c)		40-5-MDOF-A-Q
a 2-SDOF system (Figure 5 d)		40-5-MDOF-B-Q
a 2-SDOF system with non-vibrating mass (Figure 5 e)		40-5-MDOF-C-Q

4 RESULTS AND DISCUSSION

This section presents the numerical study results for load case simulation. Dynamic responses of target points under each investigated load case and load combination were evaluated to (1) determine the critical load case within the defined scope; and (2) observe the effect of a bystander on the dynamic response of a suspension pedestrian bridge.

4.1 Pedestrian load combinations

Figures 9, 10, and 11 present results for the first three load cases (1PW, 1PJ, 1PC) induced by one pedestrian (Table 4). The horizontal axis in the figures is the maximum dynamic response of each of the seven evaluated target points (Figure 8) among all responses during the entire analysis.

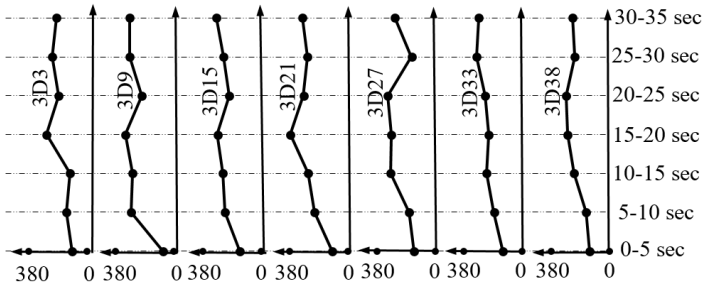

a) vertical velocity (mm/s)

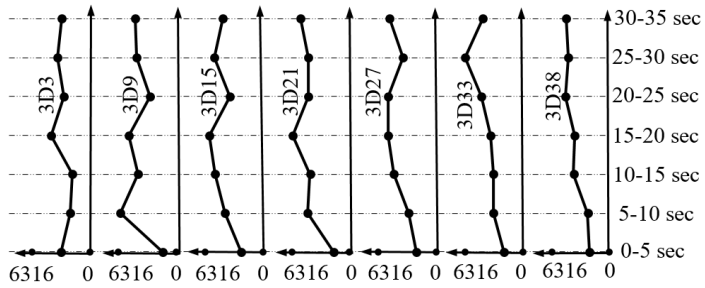

b) vertical acceleration (mm/s^2)

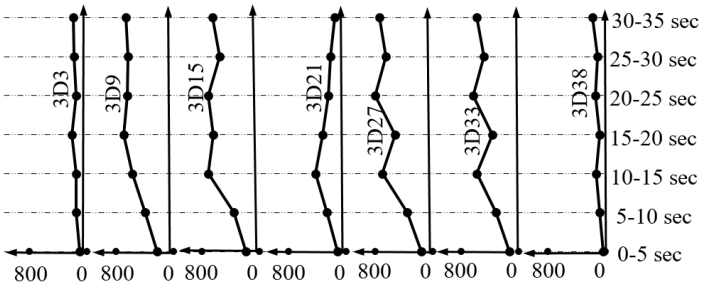

c) lateral acceleration (mm/s^2)

Figure 9. Dynamic response for a pedestrian walking across the 40-5 bridge

Figure 9 presents dynamic responses due to a walking pedestrian. Normal walking speed is 1.2 m/s; thus, a walking pedestrian takes five seconds to cross every six-meter bridge section. During the first five seconds, the walking pedestrian is in the first six-meter section, the center of which is 3D3.

From Figure 9a) it is observed that the velocity generally increases as the pedestrian progresses along the bridge and then decreases as the pedestrian approaches the end. The largest response occurs at target point 3D21 that is near the midpoint of the bridge. This response occurs when the pedestrian arrives at the bridge midpoint. The bridge responds similarly during other time periods; for example, during the 5 – 10 second period, the largest response occurs in the second, six-meter section, 3D9, as expected because the pedestrian is the forcing function acting on the structure. All predicted vertical velocities exceed the serviceability limit (32 mm/s) with the largest velocity being twelve times the limit.

From Figure 9b), the variation of bridge vertical acceleration is similar to that of the vertical velocity. Initial vertical accelerations are mostly within the serviceability limit (2250 mm/s^2); however, accelerations as the pedestrian advances exceed the limit, and in some cases are nearly three times the serviceability limit. Predicted lateral accelerations were below the serviceability limit (1800 mm/s^2) for all target points for all pedestrian positions. This is due to a much smaller force magnitude in the lateral direction.

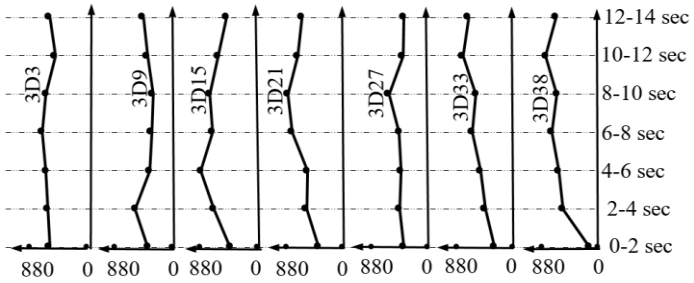

a) vertical velocity (mm/s)

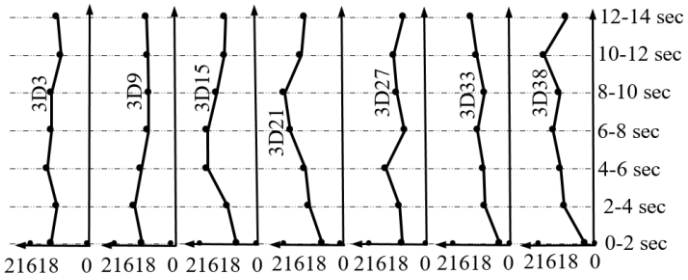

b) vertical acceleration (mm/s^2)

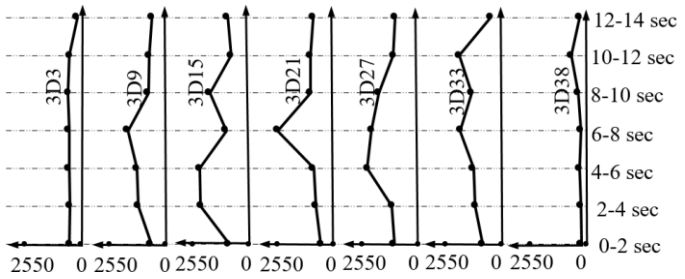

c) lateral acceleration (mm/s^2)

Figure 10. Dynamic response for a pedestrian jogging across the 40-5 bridge

Figure 10 presents the bridge dynamic response for a pedestrian jogging across the bridge. Normal jogging speed is 3 m/s; thus, a jogging pedestrian requires two seconds to pass a six-meter section. From Figure 10 it can be observed that the largest vertical velocity again occurs near the middle of the bridge; however, it occurs five seconds after the jogger passes the midpoint due to differences in load functions for the jogging force and the walking force. The peak velocity observed under the jogging load is 2.2 times the peak velocity under the walking load. This was expected because in the vertical direction, the peak jogging force is 2.5 times the peak walking as presented in Figure 1 and Figure 2. For lateral accelerations, some exceed the serviceability limit (1800 mm/s^2); however, compared to the vertical responses, lateral responses are not a significant issue for this load case.

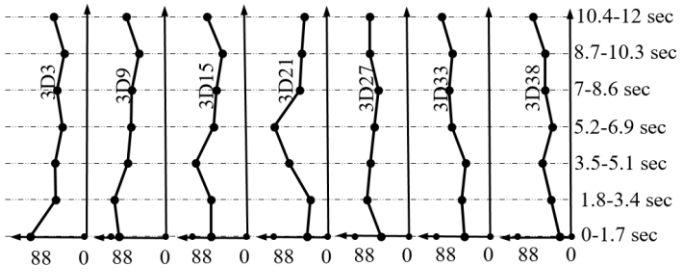

a) vertical velocity (mm/s)

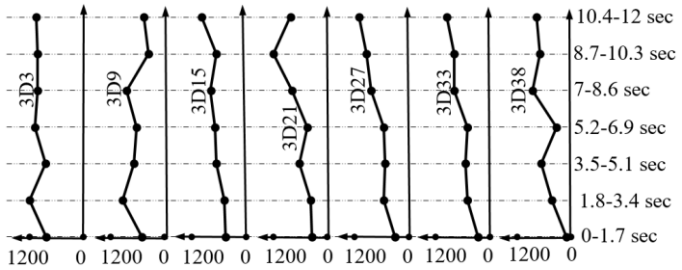

b) vertical acceleration (mm/s^2)

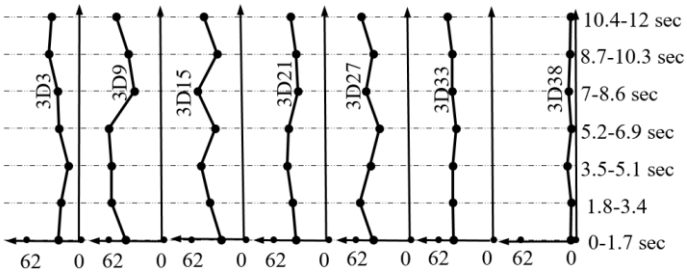

c) lateral acceleration (mm/s^2)

Figure 11. Dynamic response for a pedestrian cycling across the 40-5 bridge

Figure 11 presents the dynamic response due to a cycling pedestrian. The largest vertical velocity caused by cycling is 77 percent less than the walking load case and the largest lateral acceleration is 92 percent less. This decrease is due to the impact nature of a walking footfall force as compared to the constant but moving cycling force. The largest vertical velocity exceeds the serviceability limit (32 mm/s) by 64 percent, however, the vertical and lateral accelerations are below the limits.

Among the three pedestrian load cases studied, jogging creates the largest dynamic responses with vertical velocity consistently the major issue. Cycling does not induce a response above comfort limits, therefore, only walking and jogging forces are considered for load combinations. Due to the similar trends between vertical velocity and acceleration responses, only vertical velocities were evaluated for the load combinations.

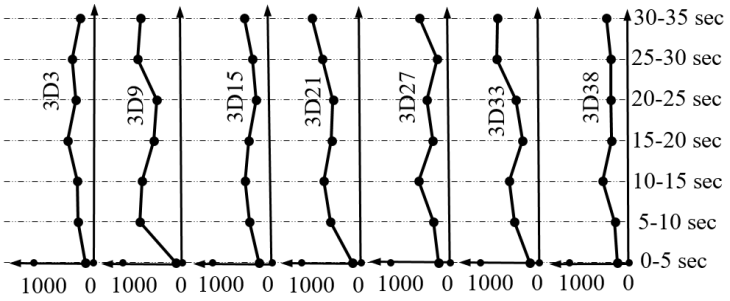

a) dynamic response in vertical velocity for the combination of 40-5-2WS-1 (mm/s)

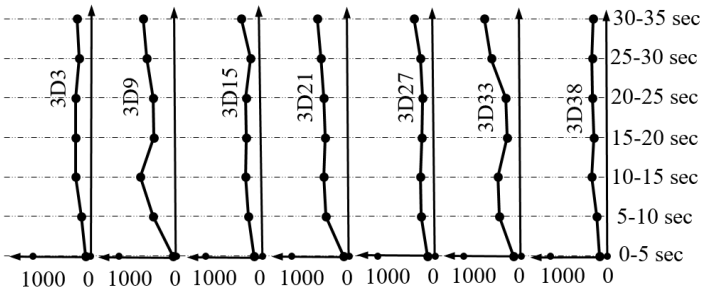

b) dynamic response in vertical velocity for the combination of 40-5-2WS-3 (mm/s)

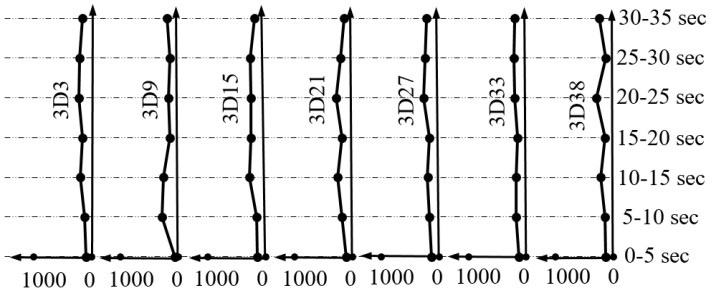

c) dynamic response in vertical velocity for the combination of 40-5-2WS-5 (mm/s)

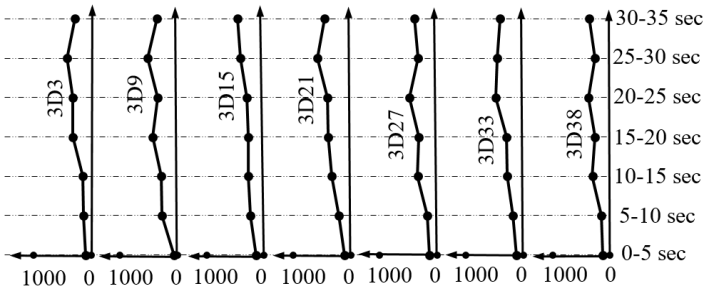

d) dynamic response in vertical velocity for the combination of 40-5-2WS-8 (mm/s)

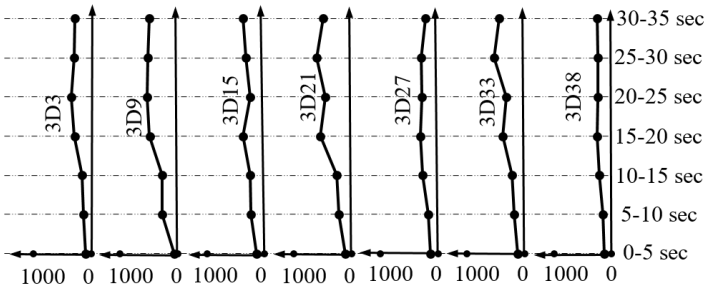

e) dynamic response in vertical velocity for the combination of 40-5-2WS-12 (mm/s)

Figure 12. Dynamic response for the load combination of two walking pedestrians crossing the bridge from the same end

Figures 12 through 15 present dynamic responses for each of the investigated load combinations (Table 4). The horizontal axis is the dynamic response of each evaluated bridge target point.

Figure 12 presents the dynamic response due to 2WS. Observing from a) through c), the vertical velocity tends to decrease significantly as the time offset increases from one second to five seconds. In c), the peak velocity is 22 percent less than that for one pedestrian. Understanding that each walking pedestrian induces a wave with the same shape, the time offset will result in either constructive or destructive action of the waves. As the time offset increases, the constructive effect dissipates. When the time offset reaches five seconds, the two waves nearly cancel, resulting in a 57 percent smaller dynamic response than a single walking pedestrian. As observed from d) and e), a further increased time offset results in constructive action.

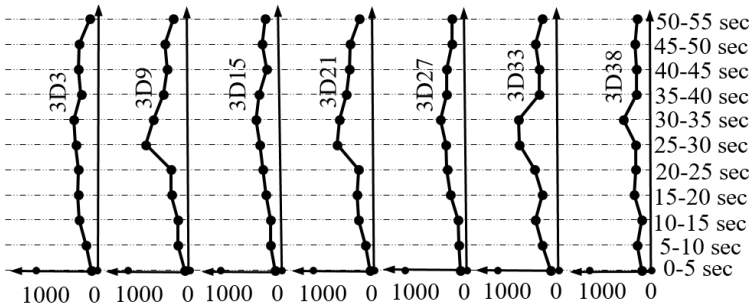

a) dynamic response in vertical velocity for the combination of 40-5-2WD-9 (mm/s)

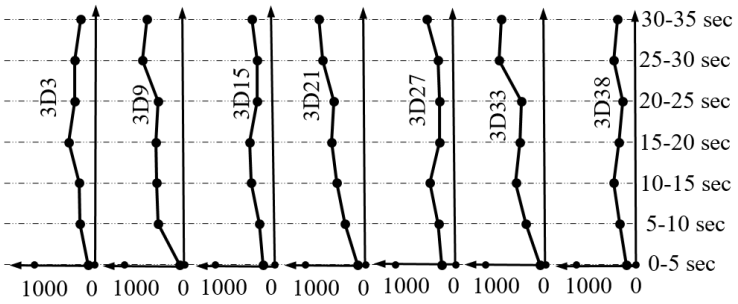

b) dynamic response in vertical velocity for the combination of 40-5-2WD-21 (mm/s)

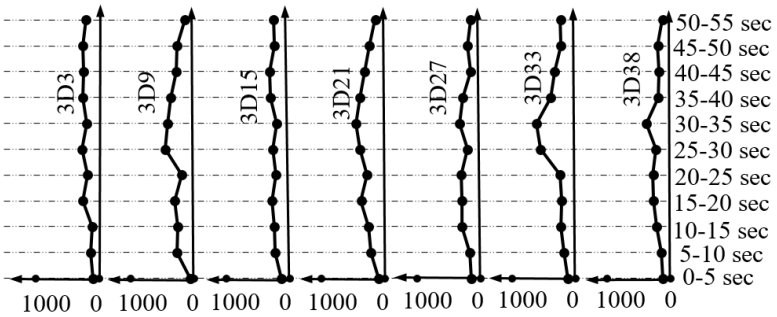

c) dynamic response in vertical velocity for the combination of 40-5-2WD-33 (mm/s)

Figure 13. Dynamic response for the combination of two walking pedestrians crossing the bridge from different ends

Figure 13 presents the dynamic response due to 2WD. The largest vertical velocity occurs at the midpoint when two pedestrians meet at 3D21, as shown in b). The largest vertical velocity is 823 mm/s for the combination 2WS and 781 mm/s for the combination 2WD. This similar magnitude is to be expected due to the symmetry of a pedestrian walking from the left to right and right left.

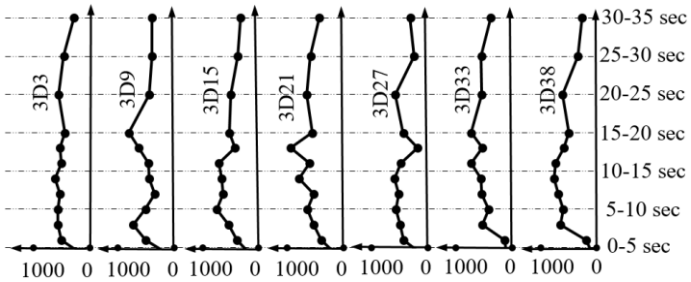

a) dynamic response in vertical velocity for the combination of 40-5-WJS-9 (mm/s)

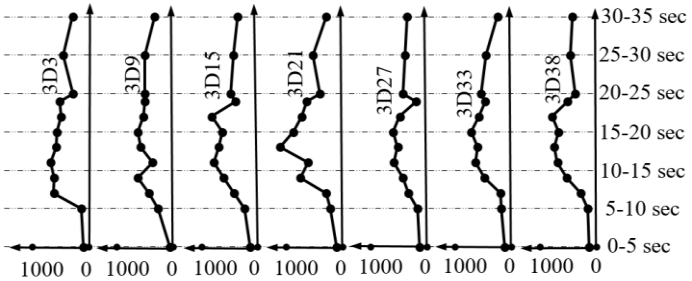

b) dynamic response in vertical velocity for the combination of 40-5-WJS-21 (mm/s)

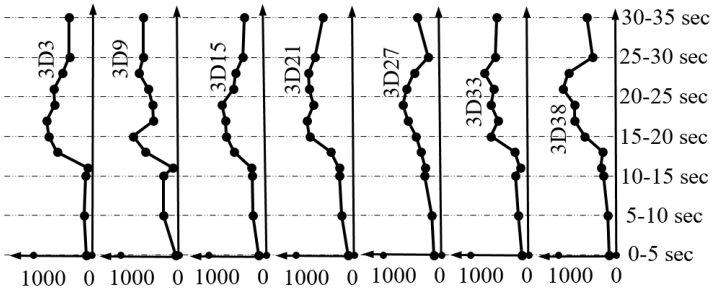

c) dynamic response in vertical velocity for the combination of 40-5-WJS-33 (mm/s)

Figure 14. Dynamic response for the combination of one walking pedestrian and one jogging pedestrian crossing the bridge from the same end

Figure 14 presents the dynamic responses due to WJS. From Figures 14a) through c), it is observed that the midpoint always experiences a large velocity. This occurs when the jogger overtakes the walker at the same location. The two pedestrians meet at 3D9, which means the jogger overtakes the walker early during in the analysis.

After the meeting, the distance between the two pedestrians increases and the jogger exits the bridge ten seconds before the walker, resulting in the small response during the last seconds. Conversely, in c), during the first several seconds, the response is relatively small, but at the end of the analysis, the responses are large. The largest vertical velocity in c) is 1104 mm/s, however, all other maximum velocities are less than 900 mm/s.

Figure 15 presents the dynamic response due to WJD. The largest velocity occurs at the midpoint when pedestrians meet at 3D21, as presented in b). Because the jogger starts from the right end of the bridge, he must begin early if the meeting is to be in the vicinity of 3D9. This results in the large velocities during the first two time periods in a). Conversely, as observed in c), large velocities occur during the last three time periods.

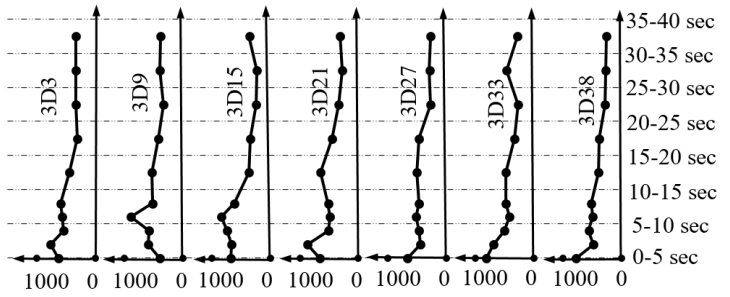

a) dynamic response in vertical velocity for the combination of 40-5-WJD-9 (mm/s)

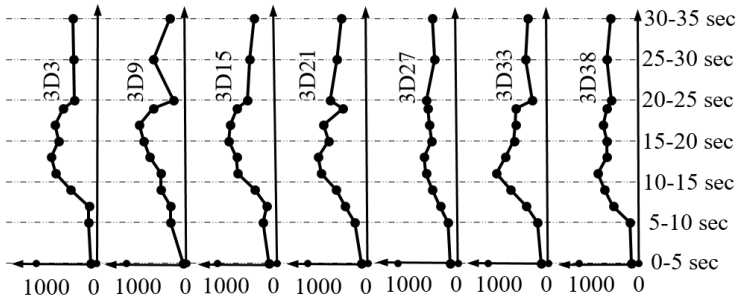

b) dynamic response in vertical velocity for the combination of 40-5-WJD-21 (mm/s)

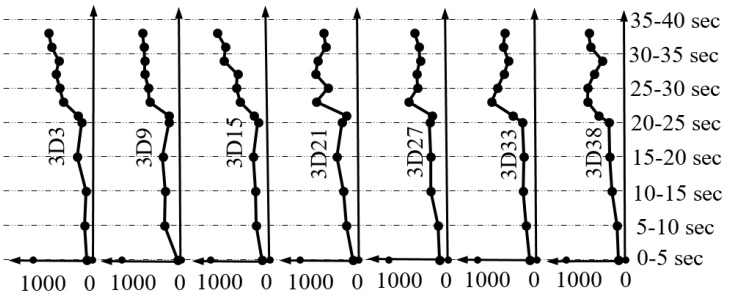

c) dynamic response in vertical velocity for the combination of 40-5-WJD-33 (mm/s)

Figure 15. Dynamic response for the combination of one walking pedestrian and one jogging pedestrian crossing the bridge from different ends

4.2 Animal load and handcart load combinations

Figures 16 and 17 present dynamic responses due to animal load and handcart load combinations (see Table 5). All dynamic responses are presented graphically with the same scale. The responses of all investigated load combinations are compared the pedestrian load combinations responses.

Figure 16 presents the dynamic response due to the animal load case. Generally, the bridge response to the animal load case is lower than the pedestrian walking case. This is largely the result of the animal modeled as the same weight as the pedestrian, where the animal maximum footfall force

magnitude during a single limb load is smaller than the animal self-weight. Therefore, the animal load combination, for a smaller animal, is not critical compared to pedestrian load combinations.

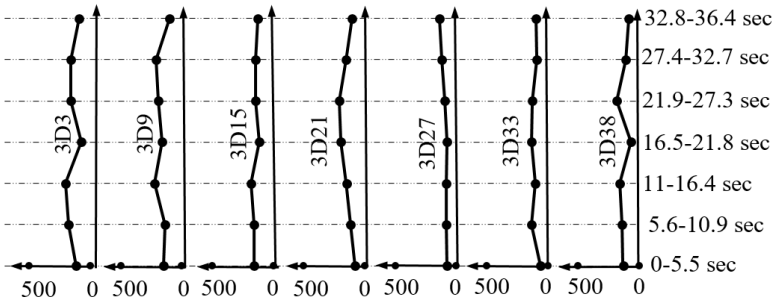

Figure 16. Dynamic responses for the animal load combination

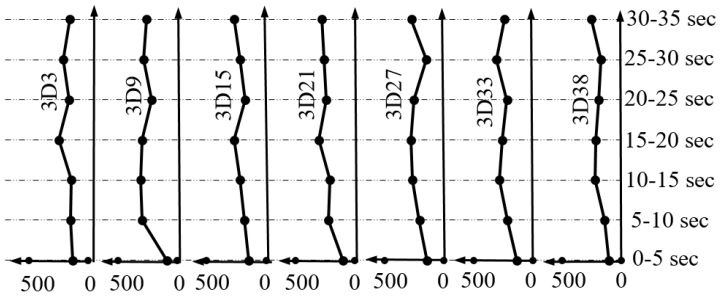

Figure 17. Dynamic responses for the handcart load combination

Figure 17 presents the dynamic response due to a pedestrian pushing a handcart. Compared to the walking pedestrian load case, the peak velocity at the midpoint decreases from 379 mm/s to 300 mm/s. This is as anticipated because responses induced by a wheeled, moving load are small, as discussed with respect to Figure 11, and tend to destructively interact with the footfall induced motions. Therefore, a pedestrian walking force controls over a pedestrian pushing a handcart.

4.3 Parametric study on bystanders

Figures 18 and 19 present dynamic responses due to a bystander model study. Six bystander models, including the five damped systems presented in Figure 5 and a simple, lumped mass, were investigated. The resulting bystander affected responses are compared to response data of the bridge without a bystander.

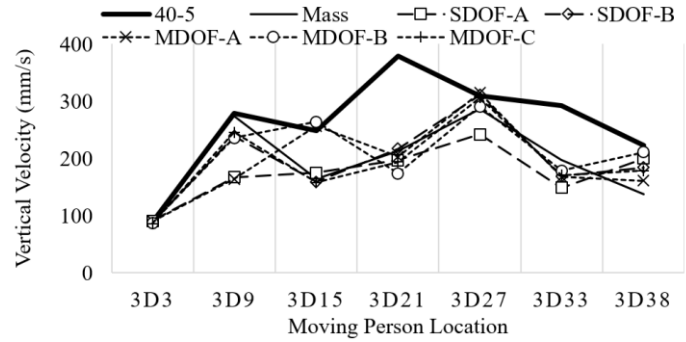

a) vertical velocity

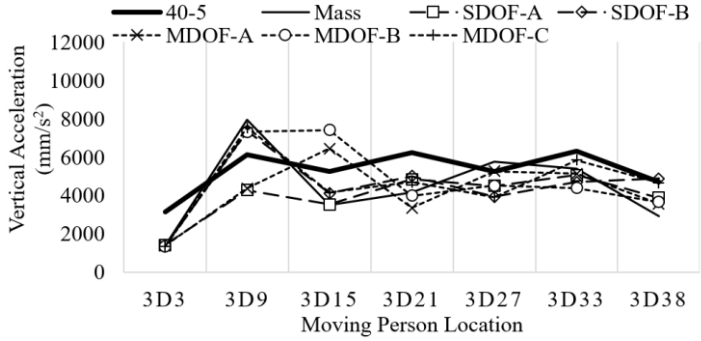

b) vertical acceleration

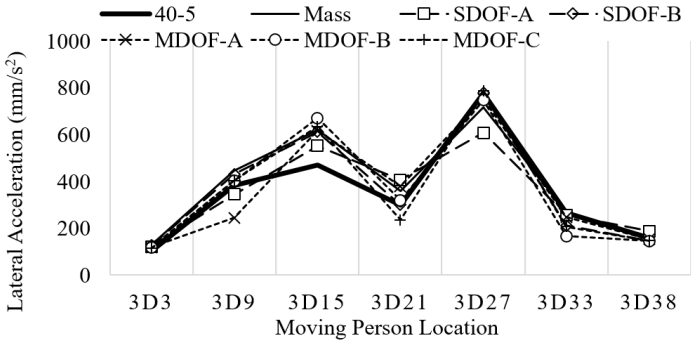

c) lateral acceleration

Figure 18. Dynamic response for 40-5 bridge with different bystander models at midpoint

Figure 18 presents bridge responses as affected separately by each of the bystander models positioned at the bridge midpoint. Comparing to the response of the load case without a bystander, both the vertical velocity and vertical acceleration decrease significantly near the location of the bystander, with a larger decrease in velocity, primarily due to damping being directly related to velocity. Responses as affected by the different bystander models, particularly vertical acceleration, are somewhat dispersed. The damped bystander models

were developed by others on the basis of a match with experimental results. However, the experiments were primarily conducted for building floor systems, which may contribute to the range of results presented here given the significant difference in both structure and human reaction. Moreover, there is little difference between the dynamic responses as affected by modeling the bystander as a mass only or as a damped system.

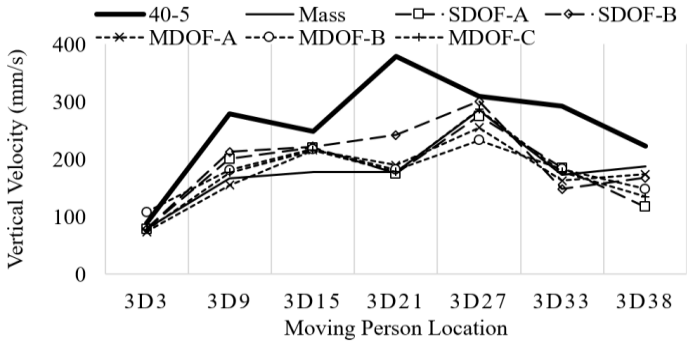

a) vertical velocity

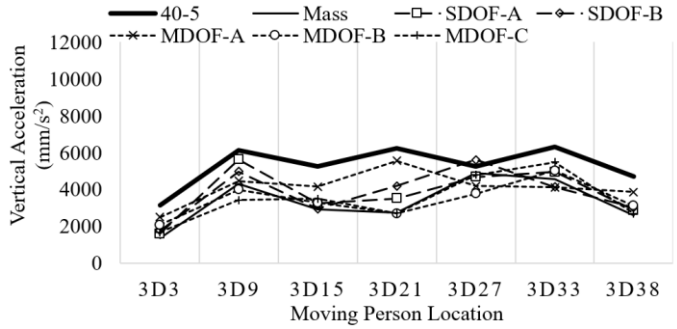

b) vertical acceleration

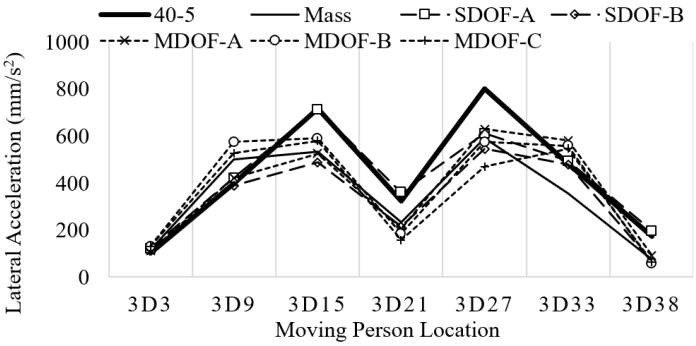

c) lateral acceleration

Figure 19. Dynamic response for 40-5 bridge with different bystander models at quarter-point

This is in large part because the pedestrian bridge studied is of very low mass and the bystander mass is relatively significant by comparison -- the increased mass of the bystander dominates over the bystander damping influence. Observed from Figure 18 c), the lateral acceleration is minimally affected by the existence of a bystander.

Figure 19 presents the dynamic response results as affected by a bystander at the bridge quarter-point. Both the vertical velocity and vertical acceleration are decreased as compared to a mid-span bystander. With a bystander present, the largest vertical responses generally occur at 3D27, far from the bystander. The lateral acceleration is again not greatly affected.

5 CONCLUSIONS

The present study utilized a scaled, physical bridge model to calibrate the numerical modeling methodology of full-scale numerical bridge models built in SAP2000. The calibrated numerical modeling methodology was applied to numerical models that enabled completion of the subsequent dynamic load case simulations. A nonlinear, direct-integration, time history analysis was conducted to determine the dynamic responses under each defined load scenario. The present study focused on multiple pedestrian loads, animal walking load, handcart load and effects of six bystander models. Conclusions drawn from the numerical simulations are as follows:

- Vertical dynamic responses are consistently the primary serviceability issue as compared to lateral response.
- A rolling load (bicycle) induces a 77 percent lower response than a walker, therefore, the cycling load case is not a significant load case when compared to pedestrian walking and jogging load case.
- When two walkers proceed side-by-side, a larger bridge dynamic response is induced, nearly double the response induced by a single walker.
- When a second walker begins two, three or four seconds after the first walker, the bridge dynamic response tends to decrease. When the time offset increases to five seconds, the dynamic response drops below the response induced by one walker.
- When a walker and a jogger start from the same end, the largest vertical velocity always occurs at the location where the jogger passes the walker. When a walker and a jogger start from opposite ends, the largest vertical velocity always occurs at the meeting location.
- The largest dynamic response induced by a load case with walker and a jogger starting from opposite ends is very similar to that induced by two walkers starting from different ends.
- The animal walking load case and the handcart load case does not induce large dynamic responses as compared to a single walker load case.
- There is little difference between responses as affected by the differences in

modeling a bystander as a mass only or as a damped system.

- The vertical dynamic response near the location of a bystander decreases significantly as compared to the same situation without a bystander; however, the lateral response is not greatly affected by the existence of a bystander.

ACKNOWLEDGMENTS

The authors gratefully acknowledge the contributions of Mr. Dave Faulds, Mr. Dan Fura, Dr. Ali Memari, Dr. Gordon Warn to the success of this study.

REFERENCES

[1] TP Andriacchi, et al. (1977). "Walking speed as a basis for normal and abnormal gait measurements." Journal of biomechanics 10(4): 261-268.
[2] John E Wheeler (1982). "Prediction and control of pedestrian-induced vibration in footbridges." Journal of the structural division 108(ST-9).
[3] FW Galbraith and MV Barton (1970). "Ground Loading from Footsteps." The Journal of the Acoustical Society of America 48(5B): 1288-1292.
[4] (Computers & Structures Inc. 2015). "CSI Analysis Reference Manual For SAP2000, ETABS, SAFE and CSiBridge."
[5] Maarten F Bobbert, et al. (2007). "Validation of vertical ground reaction forces on individual limbs calculated from kinematics of horse locomotion." Journal of Experimental Biology 210(11): 1885-1896.
[6] HW Merkens, et al. (1993). "Ground reaction force patterns of Dutch Warmblood horses at normal trot." Equine veterinary journal 25(2): 134-137.
[7] Regina Sachse (2003). The influences of human occupants on the dynamic properties of slender structures, University of Sheffield.
[8] Rolf R Coermann (1962). "The mechanical impedance of the human body in sitting and standing position at low frequencies." Human Factors: The Journal of the Human Factors and Ergonomics Society 4(5): 227-253.
[9] CW Suggs, et al. (1969). "Application of a damped spring-mass human vibration simulator in vibration testing of vehicle seats." Ergonomics 12(1): 79-90.
[10] L Wei and MJ Griffin (1998). "Mathematical models for the apparent mass of the seated human body exposed to vertical vibration." Journal of sound and vibration 212(5): 855-874.
[11] Jennifer Kearney (2015). "An Analysis of the Dynamic Response of Suspension Footbridges Measured Against Human Comfort Criteria."
[12] T Kobori and Y Kajikawa (1974). "Ergonomic evaluation methods for bridge vibrations." Transactions of JSCE 6: 40-41.
[13] SI Nakamura (2003). "Field Measurements of Lateral Vibration on a Pedestrian Suspension Bridge." Structural Engineer 81(22).